This is a preprint of an article published by *Znack Publishing House* in *Light & Engineering*
Vol. 27, No. 2, pp. 88–96, 2019. https://doi.org/10.33383/2018-034

APPLICATION OF THE PHOTOMETRIC THEORY OF THE RADIANCE FIELD IN THE PROBLEMS OF ELECTRON SCATTERING

Viktor P. Afanas'ev[1], Vladimir P. Budak[1], Dmitry S. Efremenko[2], Pavel S. Kaplya[3]

[1] National research university "Moscow Power Engineering institute", Moscow, Russia
[2] Remote Sensing Technology institute, German Aerospace Center (DLR), Oberpfaffenhofen, Germany
[3] Yandex LLC, Moscow, Russia

Abstract. The physical model of the radiance field is similar in some aspects to the elementary particle transport theory under the assumptions of the classical mechanics. Disregarding the differences in the used nomenclatures, it can be shown that the transport equations for the radiance field are identical to those for the particle flux density. Since the end of the 19th century, both theories have been developing in parallel, thereby enriching each other. In other words, a breakthrough, which has been made in one theory, readily contributes to the significant progress in another one. Nowadays the accuracy achieved in the experiments with particles is close to the limit, which allows validating the relationships derived within the light scattering theory. Besides, the experiments with particles are free from uncertainties in the scattering medium, which are typical for atmospheric remote sensing applications. In this paper, a new algorithm is described, which is derived by analogies between these theories. It is applied for calculating the electron flux elastically scattered by plane-parallel layers of a solid with the strongly forward peaked phase functions. The calculations are compared against the experimental angular distributions of electrons, which are elastically reflected by the two-layer solid samples.

Keywords: Transport theory, the small-angle approximation, light scattering, electron spectroscopy, the invariant imbedding method

Introduction

The formulation of the transport theory for elementary particles is similar to the laws of the light beam propagation considered in the ray approximation framework. Moreover, these laws are valid for all classical particles, as long as they can be localized in space. The ray approximation can be regarded as a case of a more general quantum physical concept [1], in which a photon is considered as a small particle moving along a trajectory; the latter is referred to as a 'ray.' The density of the photon flux is associated with the radiance $L(\mathbf{r},\hat{\mathbf{l}})$ at the given point $\mathbf{r}$ in the direction $\hat{\mathbf{l}}$. Under this setup, the radiance field is given by the radiative transfer equation (RTE):

$$(\hat{\mathbf{l}},\nabla)L(\mathbf{r},\hat{\mathbf{l}}) = -\varepsilon L(\mathbf{r},\hat{\mathbf{l}}) + \frac{\sigma}{4\pi}\oint L(\mathbf{r},\hat{\mathbf{l}}')x(\hat{\mathbf{l}},\hat{\mathbf{l}}')d\hat{\mathbf{l}}', \quad (1)$$

here ε, σ are the extinction and scattering coefficients, respectively, while $x(\hat{\mathbf{l}},\hat{\mathbf{l}}')$ is the single scattering phase function. Initially, the RTE was introduced in [2] for a medium without scattering. In this case, for optically thin media, the RTE is reduced to the Bouguer law, i.e. exponential brightness attenuation along a ray.

The transfer equation for particles looks similar to Equation (1), namely,

$$(\hat{\mathbf{l}},\nabla)\psi(\mathbf{r},\hat{\mathbf{l}}) = -(\sigma_{el}+\sigma_{in})\psi(\mathbf{r},\hat{\mathbf{l}}) + \frac{\sigma_{el}}{4\pi}\oint\psi(\mathbf{r},\hat{\mathbf{l}}')x(\hat{\mathbf{l}},\hat{\mathbf{l}}')d\hat{\mathbf{l}}', \quad (2)$$

here $\psi(\mathbf{r},\hat{\mathbf{l}})$ is the particle flux density at the given point $\mathbf{r}$ along direction $\hat{\mathbf{l}}$, σ_{el} is the elastic scattering cross-section, while σ_{in} is the inelastic scattering cross-section.

Equations (1) and (2) can be used to determine the flux density of photons and electrons reflected by multi-layered inhomogeneous media with the underlying surface. Essentially, they are the basis for the forward modelling in the Earth remote sensing retrieval codes and in the electron spectroscopy processing algorithms (in particular, describing the process of electron lithography, determining the backscatter factor in the X-ray spectral analysis as well as analysing the X-ray photoelectron spectroscopy (XPS) and reflected electron spectroscopy (RES) data).

The description methodologies of both electron and optical scattering are based on the transport equations. Therefore, the methods designed for solving optical problems can be used in the problems related to atomic particle scattering in solids [3-5].

By using the electron spectroscopy framework, the problem of quantitative composition analysis of samples can be readily solved. However, such an analysis of the experimental data typically requires a model of multiple elastic and inelastic scattering of electrons in solids.

Retrieval of the component composition of multi-layered samples is an ill-posed problem. It incorporates the analysis of the energy spectra of emitted electrons and extracting the information of the interest. In this regard, there are additional requirements and constraints on the scattering signal modelling algorithms and their robustness.

The state-of-the-art methods of the XPS and the elastic peak electron spectroscopy (EPES) analysis are based on rather simplistic models, in which the process of multiple elastic scattering is neglected. One of the representatives of such models is the straight-line approximation (SLA) [6,7]. The main advantage of SLA-like models consists in their simplicity. However, SLA leads to a biased estimate of the scattered electron signal [8]. Essentially, the error of the SLA approach is because the elastic scattering cross section σ_{el} in the situations, which are relevant for XPS, RES, and EPES, exceeds the inelastic scattering cross section, i.e. $\sigma_{el} > \sigma_{in}$. Several techniques were developed in order to compensate the SLA bias. However, they are *ad hoc* and do not take rigorously into account all the factors that cause the methodological errors. Unlike in remote sensing applications, in the electron scattering spectroscopy, there are several independent methods for layer-by-layer component analyses of samples. In its turn, it is possible to experimentally validate techniques which describe the reflection processes from multi-layered inhomogeneous media. Besides, it is possible to control the composition of the sample under study, even at the stage of its preparation. In this regard, layer-by-layer composition retrieval based on the analysis of electron spectra can be performed by using techniques provided by the radiative transfer theory. In this paper, it will be shown that the experimental data on angular distributions of elastically reflected electrons [9–11] is beneficial for validation of the radiation codes and models used in the Earth remote sensing operational algorithms [12–15]. The similar ideas were behind the verification study [16].

The invariant imbedding method was proposed by Ambartsumian in the 40s of the last century to describe the processes of radiation transfer in the atmospheres of stars and planets [17,18]. Essentially, this method converts the RTE for the radiance into the equations for the reflection and transmission coefficients of a slab. The method was further developed in the works of Chandrasekhar, Sobolev, and others [19, 20], primarily, for spherical and Rayleigh single scattering phase functions [17–20]. In these cases, an iterative procedure appeared to be efficient. As the first approximation, a single scattering solution was used [18]. Typically, four iterations were enough to achieve the convergence. However, strongly forward peaked phase functions with dominant small-angle scattering are of great practical importance. In particular, these are the cases relevant for electron scattering in solids and photon scattering in a turbid medium. In this paper, it will be shown that in the case of dominant small-angle scattering it is possible to simplify the solution procedure since the nonlinear Chandrasekhar equations can be linearized.

The forward peaked phase functions were considered by Gaudsmith and Saunderson [21,22] to solve the electron transport equation by using the small-angle approximation and the spherical harmonics method. Let us consider an infinite medium with the sources of light (or particles) placed in the center (the medium boundary is placed at $z = 0$); the source satisfies the following condition: $L(z = 0, \hat{\mathbf{l}}) = \delta(\hat{\mathbf{l}} - \hat{\mathbf{l}}_0)$. In [23] Scott developed a technique for solving transport equations by using the small-angle approximation. Dashen [3] applied the Ambartsumian equation, which solves the boundary problem of reflection from a semi-infinite medium, to describe the electron scattering process. Successful attempts to solve the linearized Ambartsumian and Chandrasekhar equations in the small-angle approximation were made in [4,24]. Throughout the paper, the small-angle approximation is associated with the following small parameter

$$x(\pi) / x(0) \ll 1. \tag{3}$$

In this paper, the small-angle approximation is used to derive analytical expressions for radiation reflection processes both from a semi-infinite layer and from layers of finite thickness. The small-angle solutions of the Chandrasekhar equation for the transmission function will be given. It will be shown that the small-angle approximation can be used only for Chandrasekhar equations (written for the transmission function [19]), but not for the alternative formulation from [25]. An iterative procedure will be constructed that solves the problem of reflection from multilayer samples with an underlying surface at the bottom.

The main advantage of approximate analytical solutions consists in the high computational speed, which is a prerequisite for solving inverse problems by the fitting procedure. Note that the latter is the most robust approach to deal with ill-posed problems of mathematical physics, namely, remote sensing retrieval and quantitative composition analysis using electron spectroscopy [26, 27].

The paper will present methods for the numerical solution of the Chandrasekhar equations. Currently, Monte-Carlo (MC) simulations [28, 29] are mainly used to describe the energy and angular spectra of electrons. However, MC codes require much computational time: e.g., on a standard laptop, this time ranges up to several minutes; whereas the same simulations but based on the numerical solution of the Chandrasekhar equations, presented in this paper, are performed within fractions of a second. Note, that the idea of using numerical methods to interpret the spectra of electron spectroscopy is inherited from the radiative transfer theory.

The approbation of the approximate small-angle methods developed in this work is performed by using a comparison with exact numerical solutions as well as with the experimental data.

Chandrasekhar equations for reflection and transmission functions, linearization procedure, solution by using the small-angle approximation

The equation for the reflection function derived by Chandrasekhar [19] for a layer of finite thickness reads as follows:

$$\begin{aligned}&\frac{\partial}{\partial\tau}\rho_m(\tau,\mu,\mu_0)+\left(\frac{1}{\mu}+\frac{1}{\mu_0}\right)\rho_m(\tau,\mu,\mu_0)=\Lambda x_m(\mu,\mu')+\Lambda\int_0^1 x_m(\mu,\mu')\rho_m(\tau,\mu',\mu_0)\frac{d\mu'}{\mu'}+\\&+\Lambda\int_{-1}^0 \rho_m(\tau,\mu,\mu')x_m(\mu',\mu_0)\frac{d\mu'}{\mu'}+\Lambda\int_0^1\int_{-1}^0 \rho_m(\tau,\mu,\mu')x_m(\mu',\mu'')\rho_m(\tau,\mu'',\mu_0)\frac{d\mu'}{\mu'}\frac{d\mu''}{\mu''},\end{aligned} \tag{4}$$

where τ is the dimensionless layer thickness, m is the azimuthal expansion index, ρ is the reflection function, x is the single scattering phase function, $\Lambda = \sigma_{el} / (\sigma_{el} + \sigma_{in})$ is the single scattering albedo. Consider the azimuthal expansion

$$\rho(\tau,\mu,\mu_0,\varphi-\varphi_0)=\sum_m \rho_m(\tau,\mu,\mu_0)\exp\left[im\left(\varphi-\varphi_0\right)\right], \tag{5}$$

with ϑ_0=arccos μ_0, φ_0 and ϑ =arccos μ, φ being the polar and azimuth angles of probing and viewing angles, respectively; the polar angles are defined with respect to the axis, which is perpendicular to the sample surface and looks towards the surface.

Similar to Equation (4), the equation for the transmission function *T* reads as follows:

$$\frac{1}{\mu}T_m(\tau,\mu,\mu_0)+\frac{\partial T_m(\tau,\mu,\mu_0)}{\partial\tau}=\Lambda\exp\left(-\frac{\tau}{\mu_0}\right)x_m(\mu,\mu_0)+\Lambda\int_0^1 x_m(\mu,\mu')T_m(\tau,\mu',\mu_0)\frac{d\mu'}{\mu'}+$$
$$+\Lambda\exp\left(-\frac{\tau}{\mu_0}\right)\int_0^{-1}\rho_m(\tau,\mu,\mu')x_m(\mu',\mu_0,\varphi'-\varphi_0)\frac{d\mu'}{\mu'}+ \quad (6)$$
$$+\Lambda\int_0^{-1}\int_0^1\rho_m(\tau,\mu,\mu')x_m(\mu',\mu'',\varphi'-\varphi'')T_m(\tau,\mu'',\mu_0,\varphi''-\varphi_0)\frac{d\mu'}{\mu'}\frac{d\mu''}{\mu''}.$$

Numerical solution for reflection and transmission functions

We note that the methods discussed in this section were first developed for solving the problems of radiative transfer and significantly enriched the theory of electron transfer as well. To get the matrix form of equation (1), the continuous dependency on μ' should be replaced with a discrete set of *N* values μ_i', while the integrals should be represented through the quadrature formulas. Then the reflection function S^m turns into a matrix of dimension $N\times N$, where s_i are the weights of the quadrature method, μ_i' are the quadrature nodes for the cosines of the incidence/observation angles, $w=\mathrm{diag}\,(s_i/\mu_i)$.

Bearing that in mind, equation (4) takes the following form:

$$\frac{\partial}{\partial\tau}\rho^m(\tau)+A\rho^m(\tau)+\rho^m(\tau)A=C+\rho^m(\tau)D\rho^m(\tau), \quad (7)$$

with $A=\mathrm{diag}(1/\mu)-\Lambda x^{m+}w,\ C=\Lambda x^{m-},\ D=\Lambda w x^{m-}w$.

The index + in the phase function is related to the process in which the propagation direction after the scattering event is preserved, while the index - indicates that the upward propagation changes into downward one and vice versa.

Equation (7) is referred to as the differential algebraic Riccati equation [30,31]. It can be solved numerically by several numerical techniques [31–33]. In this paper, we use the BDF (Backward Differential Formula) method [34]. The situation is somewhat simplified since the matrix x^{m+} is symmetric.

Having performed a similar discretization for particles elastically scattered inside a layer, we obtain the following matrix equation for the transmission function:

$$\frac{\partial}{\partial\tau}T_0^m(\tau)+A'T_0^m(\tau)=C, \quad (8)$$

with $A'=\mathrm{diag}\left(\frac{1}{\mu}\right)-\Lambda x^{m+}w-\Lambda\rho_0^m(\tau)wx^{m-}w,\ C=\Lambda\left(x^{m+}+\rho_0^m(\tau)wx^{m-}\right)\mathrm{diag}\left(\exp\left(-\frac{\tau}{\mu}\right)\right)$.

Let us find the solutions of the equations obtained, considering the nonlinear terms, and the solutions of the linearized matrix equations based on the BDF method. For elastic scattering we use the Henyey-Greenstein phase function, which is well-known in optics. The numbers in Figures 1 and 2 show the value of the asymmetry parameter g, which determines the degree of elongation of the Henyey-Greenstein phase function

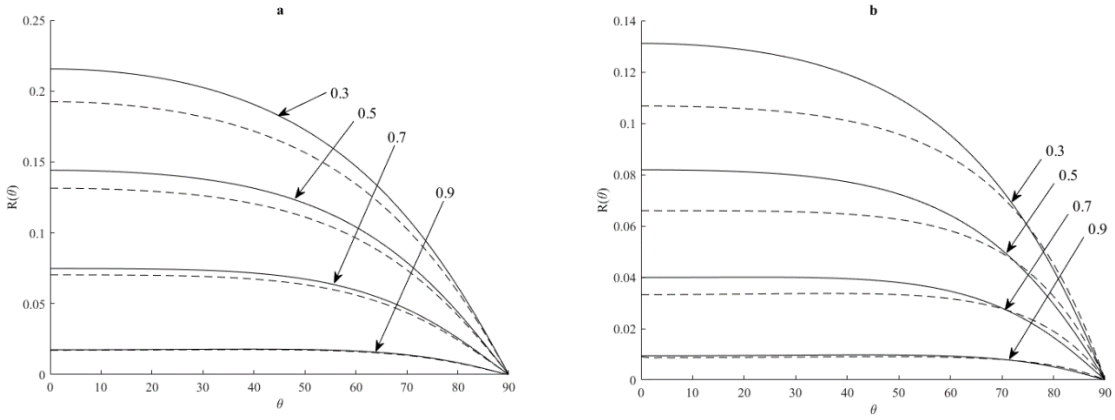

Figure 1 The reflection functions for the semi-infinite medium. The normal angle of incidence. The calculations are performed for the Henyey-Greenstein phase function. Plot (a) shows the influence of the non-linear term on the reflection function. Plot (b) illustrates the increase of error of the small-angle approximation with the phase function smoothness. The solid line is the numerical solution (MDOM), the dashed line is the small-angle approximation. The normal angle of incidence. The single scattering albedo is 0.67. Numbers with arrows are the asymmetry parameters of the Henyey-Greenstein phase function.

$$x_{HG}(\mu) = \frac{1-g^2}{(1+g^2-2g\mu)^{3/2}} = \sum_{l=0}^{\infty}(2l+1)g^l P_l(\mu), \tag{9}$$

where P_l are the Legendre polynomials.

The solution of equation (7) (and consequently, equation (4)) is shown in Figure 1 with solid lines, while the dashed line depicts the solution to equation (7) with non-linear term neglected (i.e., the second term on the right-hand side). The plots in Fig. 1 reveal the increasing of the computation error of the linearized equations. That is quite an expected result since the phase functions with $g \le 0,5$ do not have a dominant small-angle scattering part. However, even in case of violation of condition (3), the linearized equations provide a result with an error less than 10%.

In Figure 2, the solid lines represent the solution of equation (8), the dashed line shows the solution of equation (8) with neglected terms containing $\rho_0^m(\tau)$. In other words, this is a solution to equation (6), in which the last two terms on the right-hand side are neglected.

Analytical solutions of linearized equations for the reflection and transmission functions

The analysis performed on the basis of numerical solutions indicates that for strongly forward peaked phase functions (see condition (3)), the processes of reflection and transmission through the layer can be described by using the following equations:

$$\frac{\partial}{\partial\tau}\rho_m(\tau,\mu,\mu_0)+\left(\frac{1}{\mu}+\frac{1}{\mu_0}\right)\rho_m(\tau,\mu,\mu_0)=\Lambda x_m(\mu,\mu')+\Lambda\left(\frac{1}{\mu}+\frac{1}{\mu_0}\right)\int_0^1 x_m(\mu,\mu')\rho_m(\tau,\mu',\mu_0)\frac{d\mu'}{\mu'} \tag{10}$$

and

$$\frac{1}{\mu}T_m(\tau,\mu,\mu_0)+\frac{\partial T_m(\tau,\mu,\mu_0)}{\partial\tau}=\Lambda\exp\left(-\frac{\tau}{\mu_0}\right)x_m(\mu,\mu_0)+\Lambda\int_0^1 x_m(\mu,\mu')T_m(\tau,\mu',\mu_0)\frac{d\mu'}{\mu'}. \tag{11}$$

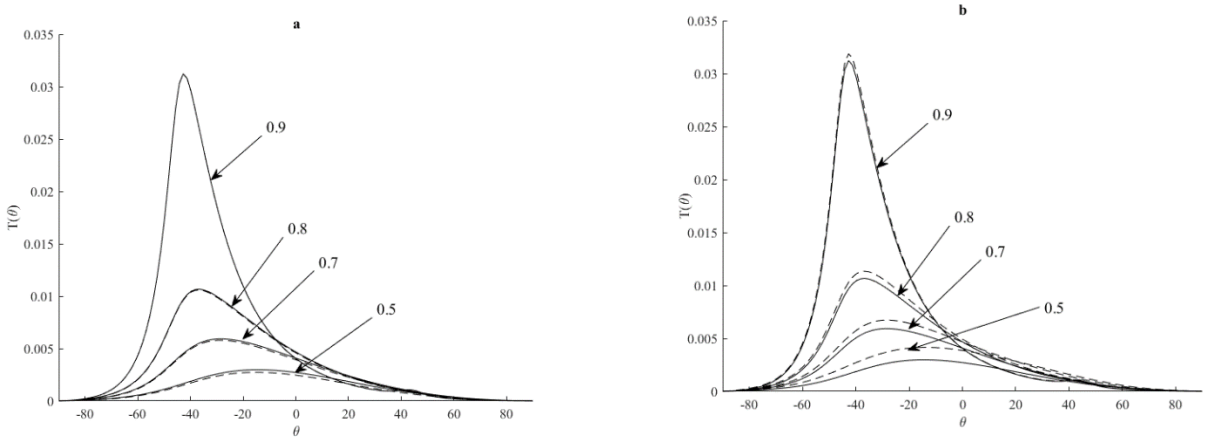

Figure 2. The transmission functions for the layers of thickness 0.1 l_{tr} . Plot (a) shows the influence of the non-linear term. The solid line is the result with the non-linear term, while the dashed line shows the result without non-linear term taken into account. Plot (b) shows the increasing of the small-angle approximation error with the smoothness of the phase function. The solid line is the numerical solution (MDOM), the dashed line is the small-angle approximation. The angle of incidence is 45 °, the single scattering albedo is 0.54. Numbers with arrows are the asymmetry parameters of the Henyey-Greenstein phase function.

The method of spherical harmonics is based on the representation of functions through the Legendre polynomial series. However, to be able to apply the method of spherical harmonics (which is a standard procedure for analytic solution of equations (10) and (11)), based on the orthogonality property of the Legendre polynomials within the domain [-1,1], it is necessary to perform the analytic extension of the integrands to the domain (-1, 1). For equation (10) this step is trivial since in the domain (0, -1) the integrand goes to zero due to condition (3); the analytical continuation for equation (11) is not straightforward. There are several approaches to how to deal with this problem, (see, e.g. [2]). The most efficient implementation is given in [35, 36].

The solution of equation (11), in which the integration limits are extended into the range [-1, 1] in the integral term can be found by using the idea of Goudsmit and Saunderson: namely, in the multiplier $1/\mu$ in the first term of the left-hand side of (11) and in the exponent in the first term of the right-hand side of (11) (with respect to τ/μ_0), the values μ, μ_0 are considered to be constants. This approximation means replacing the real path by the projective one. A significant error occurs if the transport path of a photon or electron $l_{tr} = n^{-1}\left(\sigma_{el} + \sigma_{in}\right)^{-1}$ and the average electron path between elastic collisions $l_{el} = 1/\left(n\sigma_{el}\right)$ are comparable. Note that in the case of the Henyey–Greenstein phase function we have

$$l_{tr} / l_{el} = \sigma_{el} / \left(\sigma_{el} + \sigma_{in}\right) = 1/\left(1-g\right). \qquad (12).$$

The error in this case does not exceed 5%, as long as $l_{tr} / l_{el} \gg 1$.

Taking into account the assumptions made after the substitution of the Legendre polynomial expansions into equation (11), we obtain a system of separable differential equations; applying the boundary condition $T_{lm}(\tau) = 1$, the solution for the transmission function can be derived:

$$T(\tau, \mu, \mu_0) = \frac{\Lambda \mu \mu_0}{2} \sum_l \frac{2l+1}{2} x_l P_l\left(\mu_0 \to \mu\right) \cdot \left[\frac{\mathrm{e}^{-\tau/\mu} - \mathrm{e}^{-(1-\Lambda x_l)\tau/\mu_0}}{\left(\mu - \mu_0\right) - \Lambda x_l \mu} + \frac{\mathrm{e}^{-\tau/\mu_0} - \mathrm{e}^{-(1-\Lambda x_l)\tau/\mu}}{\left(\mu_0 - \mu\right) - \Lambda x_l \mu_0} \right]. \qquad (13)$$

Equation (10) is solved by the method of iterations, which provides the analytical extension in a systematic way. A detailed description of this procedure is given in [35, 36]. The final result is

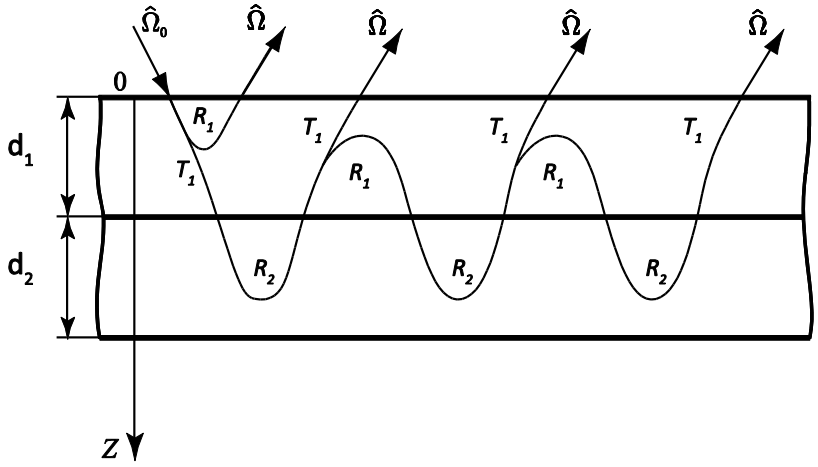

Figure 3. The two-layer model of reflection. The curved line corresponds to the reflection function, while the straight line is associated with the transmission function.

$$\rho(\tau,\mu,\mu_0)=\frac{\mu\mu_0}{\mu+\mu_0}\sum_l\frac{2l+1}{2}x_lP_l(\mu_0\to\mu)\cdot\left[E_1\left(\tau\frac{\mu+\mu_0}{\mu\mu_0}\right)-E_1\left((1-\Lambda x_l)\tau\frac{\mu+\mu_0}{\mu\mu_0}\right)-\ln(1-\Lambda x_l)\right], \quad (14)$$

where $E_1(x)=\int_x^\infty t^{-1}e^{-t}dt$ is the integral exponent.

Figures 1 and 2 illustrate the comparison between the exact numerical solution and the small-angle approximation model.

Reflection from multilayer structures

We consider reflection from multilayer structures using the angular distributions of electrons, elastically reflected from solids, as an example. In the literature, there are experimental data on the angular distributions of electrons reflected by homogeneous solids as well as by multilayer samples [9–10, 37–42].

Consider a two-layer sample (see Fig. 3). In accordance with the described scheme, the reflection function for a two-layer sample can be represented as

$$R_{12m}(\tau_1,\tau_2,\mu_0,\mu)=R_{1m}(\tau_1,\mu_0,\mu)+\int_{-1}^{1}d\mu'\int_{-1}^{1}d\mu''T_{1m}(\tau_1,\mu_0,\mu')R_{2m}(\tau_2,\mu',\mu'')T_{1m}(\tau_1,\mu'',\mu)+\ldots \quad (15)$$

or, exploiting the one-speed approximation and the small angle approximation,

$$R_{12m}(\tau_1,\tau_2,\mu_0,\mu)=R_{1m}(\tau_1,\mu_0,\mu)+\int_{-1}^{1}d\mu'T_{1m}\left(\tau_1(1/\mu_0+1/\mu),\mu_0,\mu'\right)R_{2m}(\tau_2,\mu',\mu). \quad (16)$$

The computations for three-layer systems can be performed by using the relation, which is similar to equation (16), namely,

$$R_{123lm}(\tau_1,\tau_2,\tau_3)=R_{1lm}(\tau_1)+R_{23lm}(\tau_2,\tau_3)\cdot\exp\left[-(1-\Lambda x_{lm})\tau_1\left(\mu^{-1}+\mu_0^{-1}\right)\right], \quad (17)$$

here $R_{23lm}(\tau_2,\tau_3)$ is computed by using equation (16) with the following index perturbation: $1\to 2;\ 2\to 3$.

Figure 4 shows the angular distributions of electrons, elastically reflected by the two-layer systems (the layer of Be on the Au substrate), computed by using the exact numerical solutions and the small-angle solution (16).

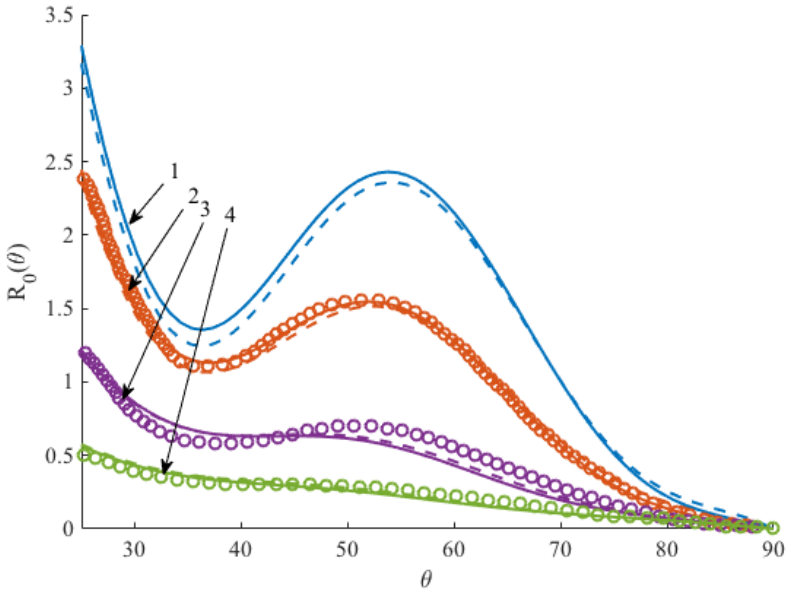

Figure 4. Angular distributions of electrons, which are reflected by the gold samples with a beryllium layer on top. The solid line corresponds to the exact numerical solution of equations (7) and (8), dashed line show the results of the small angle approximation (equations (13) and (14)), while the circles show the experimental data [10]. The computed Be layer thicknesses are: 1. 0 nm, 2. 0,5 nm, 3. 2,5 nm, 4. 3,8 nm.

Conclusion and main results

The paper has presented several analytical solutions that describe the radiance transmission and reflection in turbid media with satisfactory accuracy. The derived solutions describe radiation scattering in multi-layered inhomogeneous media. The approach developed in this work is based on the methods developed in radiative transfer for spherical and Rayleigh phase functions, as well as methods proposed by Ambartsumian, Chandrasekar, Sobolev and other remarkable scientists who solved the problems of light scattering in the atmospheres of stars and planets (see [17-20]). In the present work, it is shown that the methods designed in [17–20] are efficient in the problems when the scattering phase functions are strongly forward peaked (see condition (3)).

Analytical solutions such as (13) and (14) make it possible to perform calculations with high speed and accuracy. Given that, the error of the models as a function of the most relevant parameters (namely, the asymmetry parameter and the single scattering albedo) can be analysed.

Computational speed is an essential factor in the inverse problem solution design. For example, when the reflection function from multilayer structures is considered, we need to determine the layer thickness. Typically, it is retrieved by using the fitting method, in which the direct problem is solved several times.

Due to the integration of numerical methods of the photometric light scattering theory into electron scattering problems for determining the hydrogen isotope profiles by the elastic peak electron spectroscopy (EPES), the sensitivity of the EPES technique has been increased by order of magnitude. In fact, the sensitivity has reached almost 10 % for hydrogen isotopes in plasma faced materials [43].

Radiative transfer techniques, applied for the physical interpretation of the effects of electron and ion scattering, have brought the optical terminology (such as “brightness rotation” and “underlying surface”) into electron and ion spectroscopy [44]. The authors of this paper are confident that the presented small-angle solutions will be used for solving problems of light scattering in turbid media, as well as sea optics problems.

References

1. *Veklenko B.A.* The nature of the photon and quantum optics // Light & Engineering – 2018. – Vol. 26. – No. 2. – P.4–13.
2. *Beer A.* Bestimmung der Absorption des rothen Lichts in farbigen Flüssigkeiten // Annal. Phys. Chem. – 1852. – V.86. – P. 78–88.
3. *Dashen R.F.* Theory of electron backscattering // Phys. Rev. – 1964. – V.134. – P.1025-1032.
4. *Afanas'ev V.P., Naujoks D.* Backscattering of fast electrons // Phys. Stat. Sol. – 1990. – V.164. – P.133-140.
5. *Borodyansky S.* Effects of elastic scattering on energy spectra of emitted and backscattered electrons // Surf. Interface. Anal. – 1993. – V.84. – P.811-814.
6. *Hofmann S.* Auger- and X-Ray Photoelectron Spectroscopy in Materials Science. – Berlin/Heidelberg: Springer, 2013.
7. *Powell C.J., Jablonski A.* Progress in quantitative surface analysis by X-ray photoelectron spectroscopy: Current status and perspectives // J. of Electron Spectros. Relat. Phenom. – 2010. – V. 178-179. – P.331-346.
8. *Kaplya P.S.* Creating high-precision methods for analyzing solids on the basis of decoding electronic spectroscopic data by invariant imbedding methods // Thesis for the degree of candidate physical and mathematical of sciences. – 2016. DOI: 10.13140/RG.2.1.3428.8246 [in Russian]
9. *Bronstein I.M., Vasilyev A.A., Pronin V.P., Khinich I.I.* Elastic reflection of medium-energy electrons from disordered metal surfaces. Izvestiya AN SSSR, Ser. physical – 1985. – V.49. – № 9. – P.1755–1759. [in Russian]
10. *Bronstein I.M., Pronin V.P.* Elastic Scattering of Medium-Energy Electrons by Metal Films // Solid State Physics. – 1975. – V. 17. – P. 2431–2433. [in Russian]
11. *Gergely G.* Elastic backscattering of electrons: determination of physical parameters of electron transport processes by elastic peak electron spectroscopy // Prog. Surf. Sci. – 2002. – V.71. – P.31–88.
12. *Doicu A., Trautmann T.* Discrete-ordinate method with matrix exponential for a pseudo-spherical atmosphere: Scalar case // J. Quant. Spectrosc. Radiat. Transfer. – 2009. V. 110. – P.146-158.
13. *Spurr R.J.D., Kurosu T.P., Chance K.V.* A linearized discrete ordinate radiative transfer model for atmospheric remote-sensing retrieval // J. Quant. Spectrosc. Radiat. Transfer. – 2001. – V.68. – №6. – P.689-735.
14. *Stamnes K., Tsay S.,C., Wiscombe W., Jayaweera K.* Numerically stable algorithm for discrete-ordinate-method radiative transfer in multiple scattering and emitting layered media // Appl. Opt. – 1988. – V.27. – P.2502–2509.
15. *Budak V.P., Korkin S.V.* Complete matrix solution of radiative transfer equation for pile of horizontally homogeneous slabs // J. Quant. Spectrosc. Radiat. Transfer. – 2011. – V.112. – P.1141-1148.
16. *Afanas'ev V.P., Budak V.P., Efremenko D.S. and Lubenchenko A.V.* Angular Distributions of Electrons and Light Ions Elastically Reflected from a Solid Surface // Journal of Surface Investigation. X-ray, Synchrotron and Neutron Techniques. – 2010. – V.4. – No. 3. – P. 488–493
17. *Ambartsumyan V.A.* New method for calculating the scattering of light in a turbid medium // Izv. AN Arm. SSR, sir. geogr. and geophysics. – 1942. – I.3. – P. 97-106. [in Russian]
18. *Ambartsumyan V.A.* To the problem of diffuse reflection of light // Journal of Experimental and Theoretical Physics. – 1943. -V.13, issues.9-10. – P.323-334. [in Russian]
19. *Chandrasekhar S.* Radiative transfer. – London: Oxford University Press, 1950.
20. *Соболев В.В.* Рассеяние света в атмосферах планет. – М.: Наука, 1972. [in Russian]
21. *Goudsmit S., Saunderson J.L.* Multiple scattering of electrons // Phys. Rev. – 1940. – V.57. – P.24-29.
22. *Goudsmit S., Saunderson J.L.* Multiple scattering of electrons. II // Phys. Rev. – 1940. – V.58. – P.36-42.
23. *Scott W.* Theory of Small-Angle Multiple Scattering of Fast Charged Particles // Rev. of Modern Phys. – 1963. – V.35. – P.231-313.
24. *Afanasyev V.P.* Elementary processes and kinetics of high-temperature non-equilibrium plasma. - Moscow.: Izd. MEI, 1988. [in Russian]

25. *Ambartsumyan V.A.* On the diffuse reflection of light by a turbid medium // Reports of the USSR Academy of Sciences. – 1943. – V.38. – №8. – P.257-261. [in Russian]
26. *Afanas'ev V.P., Golovina O.Yu., Gryazev A.S., Efremenko D.S., Kaplya P.S.* Photoelectron spectra of finite-thickness layers // Journal of Vacuum Science & Technology B. – 2015. – V.33. – P.03D101.
27. *Afanas'ev V.P., Gryazev A.S., Efremenko D.S., Kaplya P.S.* Differential inverse inelastic mean free path and differential surface excitation probability retrieval from electron energy loss spectra // Vacuum. – 2017. – V. 136. – P.146-155.
28. *Werner W.S.M.* Differential probability for surface adn volume electronic excitations in Fe,Pd and Pt // Surface Science – 2005. – V. 588. – P. 26-40.
29. *Werner W.S.M.* Analysis of reflection electron energy loss spectra (REELS) for determination of the dielectric function of solids: Fe, Co, Ni // Surface Science – 2007. – V.601. – No. 10. – P. 2125-2138.
30. *Bellman R, Kalaba R, Wing G.* Invariant imbedding and mathematical physics. I. Particle processes // J. Math. Phys. – 1960. – V.1. – P.280–308.
31. *Flatau PJ, Stephens GL.* On the fundamental solution of the radiative transfer equation // J. Geophys. Res. – 1988. –V.93(D9). – P.11037–11050.
32. *Waterman P.C.* Matrix-exponential description of radiative transfer // J. Opt. Soc. Am. – 1981. – V.71(4). – P.410-422.
33. *Efremenko D.S., Molina Garcia V., Gimeno Garsia S., Doicu A.* A review of the matrix-exponential formalism in radiative transfer // J. Quant. Spectrosc. Radiat. Transfer. – 2017. – V.196. – P.17-45.
34. *Pienado J., Ibañez J., Hernández V., Arias E.* A family of BDF algorithms for solving Differential Matrix Riccati Equations using adaptive techniques // Procedia Computer Science – 2010. – V.1. – P. 2569-2577.
35. *Afanas'ev V.P., Efremenko D.S., Kaplya P.S.* Analytical and numerical methods for computing electron partial intensities in the case of multilayer systems // Journal of Electron Spectroscopy and Related Phenomena. – 2016. – V. 210. – P. 16-29.
36. *Afanasyev, V.P., Kaplya, PS, Lisitsyna, E.Yu.* Small-Angle Approximation and the Osvald-Kasper-Gaukler Model in the Problems of Electron Reflection from Solids // Surface. X-ray synchrotron and neutron studies. – 2016. – №3. – P.66-71. [in Russian]
37. *Jablonski A., Hansen H.S., Jansson C., Tougaard S.* Elastic electron backscattering from surfaces with overlayers // Phys. Rev.B. – 1992. – V.45. – P.3694-3702.
38. *Jablonski A.* Elastic electron backscattering from gold // Phys. Rev.B. – 1991. – V.43. – P.7546-7554.
39. *Jablonski A., Jansson C., Tougaard S.* Elastic electron backscattering from surfaces: Prediction of maximum intensity // Phys. Rev. B – 1993. – V.47. – P.7420-7430.
40. *Zommer L., Lesiak B., Jablonski A.* Energy dependence of elastic electron backscattering from solids // Phys. Rev.B. – 1993. – V.47. – P.13759-13762.
41. *Kuzovlev A.I., Kurnaev V.A., Remizovich V.S., Trifonov N.N.* Refraction of the beam of charged particles during inclined transmission through a thin target // Nucl. Instrum. and Methods. Research Section B: Beam Interactions with Materials and Atoms – 1998. – V.135. – P. 477-481.
42. *Bronstein I.M., Pronin V.P.* Elastic reflection of medium-energy electrons during the deposition of Be on Au // XXVIII Herzen Readings. Physical and semiconductor electronics. - Leningrad.: Publishing House of LGPI of A.I. Herzen, 1975. – P.18–20. [in Russian]
43. *Afanas'ev V.P., Gryazev A.S., Kaplya P.S., Köppen M., Ridzel O. Y., Subbotin N.Y., Hansen P.* Investigation of Deuterium Implantation into Beryllium Sample by Electron Energy Loss Spectroscopy // IOP Conf. Series: Journal of Physics: Conf. Series – 2017. – V.891. – P.012303(1-6).
44. Afanasyev V.P., Kaplya P.S. Transmission function. The effect of "turning the body of brightness" // Surface. X-ray, synchrotron and neutron studies. – 2017. – № 12. – P.66–75. [in Russian]